ELSEVIER

Engineering Analysis with Boundary Elements 31 (2007) 311–317

ENGINEERING ANALYSIS with BOUNDARY ELEMENTS

www.elsevier.com/locate/enganabound

RBF-based meshless method for large deflection of thin plates

Mahmoud Naffa[a], Husain J. Al-Gahtani[b,*]

[a]Saudi Aramco, Dhahran, Saudi Arabia
[b]King Fahd University of Petroleum and Minerals (KFUMP), Dhahran 31261, Saudi Arabia

Received 13 June 2006; accepted 5 October 2006
Available online 4 December 2006

Abstract

A simple, yet accurate, meshless method for the solution of thin plates undergoing large deflections is presented. The solution is based on the use of fifth order polynomial radial basis function to build an approximation for the solution of two coupled nonlinear differential equations governing the finite deflection of thin plates. The resulted nonlinear algebraic equations are solved using an incremental-iterative procedure. The accuracy and efficiency of the method is verified through several numerical examples.

Keywords: RBF; Meshless; Plate; Finite deflection

1. Introduction

In some applications of thin elastic plates, the deflections may increase under loading conditions beyond a certain limit recognized as large deformations. Because of these large deformations, the midplane stretches and hence produces considerable in-plane stresses that are neglected by the small-deflection bending theory. For instance, in the case of a a clamped circular plate subjected to a uniform load that produces a central deflection of 100% of its thickness, the maximum stretching stress is approximately 40% of the maximum bending stress [1]. For such situations, an extended plate theory must be employed, accounting for the effect of large deflection. Large elastic deflection of a thin elastic plate is governed by coupled nonlinear differential equations for which analytical solutions are available only for very few cases involving simple geometries and loading conditions [1–5]. For other cases, the problem has to be solved using numerical techniques such as the finite-difference method (FDM), the finite-element method (FEM) and the boundary-element method (BEM).

Nevertheless, the possibility of obtaining numerical solutions without resorting to the mesh-based techniques mentioned above, has been the goal of many researchers throughout the computational mechanics community for the past two decades or so. Radial basis function (RBF) is one of the most recently developed meshless methods that has attracted attention in recent years, especially in the area of computational mechanics [6–8]. This method does not require mesh generation which makes them advantageous for 3-D problems as well as problems that require frequent re-meshing such as those arising in nonlinear analysis. Due to its simplicity to implement, it represents an attractive alternative to FDM, FEM and BEM as a solution method of nonlinear differential equations. However, it is only since rather recently that RBF has been used to approximate solutions for partial differential equations and therefore this area is still relatively unexplored.

The roots of RBF goes back to the early 1970s, when it was used for fitting scattered data [9]. In 1982, Nardini and Brebbia [10] coupled RBF with BEM in a technique called dual-reciprocity BEM to solve free-vibration problems, where the RBF was used to transform the domain integrals into boundary integrals. Thereafter, many researchers have used RBF in conjunction with BEM to solve various problems in computational mechanics. The method, however has not been applied directly to solve partial

*Corresponding author. Tel.: +966 3 860 2900; fax: +966 3 860 2911.
E-mail address: hqahtani@kfupm.edu.sa (H.J. Al-Gahtani).

0955-7997/$ - see front matter © 2006 Elsevier Ltd. All rights reserved.
doi:10.1016/j.enganabound.2006.10.002

differential equations until 1990 by Kansa [11,12]. Since then, many researchers have suggested several variations to the original method, e.g., Refs. [13–18] not to mention many others. In general, RBF method expands the solution of a problem in terms of RBFs and chooses expansion coefficients such that the governing equations and boundary conditions are satisfied at some selected domain and boundary points. However, one of the important issues in applying this technique is the determination of the proper form of RBF for a given differential equation. Most of the available RBFs involve a parameter, called shape factor, which needs to be selected so that the required accuracy of the solution is attained. In this paper, the simple fifth order polynomial RBF that does not involve a shape factor is considered. The objective of this paper is to offer a simple mesh-free method for the solution of thin elastic plates undergoing large deflection. The method is also applicable to other nonlinear problems in various areas of computational mechanics. The paper is organized as follows. The governing equations based on w–F formulation are presented in Section 2. In Section 3, the RBF method as applied to the large deflection of thin plates is illustrated. The incremental-iterative procedure for solving the resulting RBF coupled nonlinear equations is explained in Section 4. The efficiency of the method is demonstrated by numerical examples in Section 5, followed by some concluding remarks in Section 6.

2. Governing equations

The details of the derivation of equations governing the finite deflection of thin plates are given in the classical book by Timoshenko [1]. The equations are represented here for clarity and in order to refer to them during various stages of the numerical solution.

Let us denote the membrane forces acting in the middle plane of the plate by N_x, N_y and N_{xy}. In the absence of body forces, the equations of equilibrium along x and y are given by

$$\frac{\partial N_x}{\partial x}+\frac{\partial N_{xy}}{\partial y}=0, \tag{1}$$

$$\frac{\partial N_{xy}}{\partial x}+\frac{\partial N_y}{\partial y}=0. \tag{2}$$

The third equation necessary to determine the three quantities N_x, N_y and N_{xy} is obtained from a consideration of the strain in the middle surface of the plate during bending. The corresponding strain components are

$$\varepsilon_x=\frac{\partial u}{\partial x}+\frac{1}{2}\left(\frac{\partial w}{\partial x}\right)^2, \tag{3}$$

$$\varepsilon_y=\frac{\partial v}{\partial y}+\frac{1}{2}\left(\frac{\partial w}{\partial y}\right)^2, \tag{4}$$

$$\gamma_{xy}=\frac{\partial u}{\partial y}+\frac{\partial v}{\partial x}+\frac{\partial w}{\partial x}\frac{\partial w}{\partial y}. \tag{5}$$

By taking the second derivative of these expressions and combining the resulting equations, it can be shown that

$$\frac{\partial^2\varepsilon_x}{\partial y^2}+\frac{\partial^2\varepsilon_y}{\partial x^2}-\frac{\partial^2\gamma_{xy}}{\partial x\partial y}=\left(\frac{\partial^2 w}{\partial x\partial y}\right)^2-\frac{\partial^2 w}{\partial x^2}\frac{\partial^2 w}{\partial y^2}. \tag{6}$$

By replacing the strain components by the following equivalent expressions:

$$\varepsilon_x=\frac{1}{hE}\left(N_x-\nu N_y\right), \tag{7}$$

$$\varepsilon_y=\frac{1}{hE}\left(N_y-\nu N_x\right), \tag{8}$$

$$\gamma_{xy}=\frac{1}{hG}N_{xy}, \tag{9}$$

the third equation in terms of N_x, N_y and N_{xy} is obtained. The solution of these equations is greatly simplified by the introduction of a stress function F. It may be seen that Eqs. (1) and (2) are identically satisfied by taking

$$N_x=h\frac{\partial^2 F}{\partial y^2},\quad N_y=h\frac{\partial^2 F}{\partial x^2},\quad N_{xy}=-h\frac{\partial^2 F}{\partial x\partial y}, \tag{10}$$

where F is a function of x and y. If these expressions for the forces are substituted in Eqs. (7)–(9), the strain components become

$$\varepsilon_x=\frac{1}{E}\left(\frac{\partial^2 F}{\partial y^2}-\nu\frac{\partial^2 F}{\partial x^2}\right), \tag{11}$$

$$\varepsilon_y=\frac{1}{E}\left(\frac{\partial^2 F}{\partial x^2}-\nu\frac{\partial^2 F}{\partial y^2}\right), \tag{12}$$

$$\gamma_{xy}=-\frac{2(1+\nu)}{E}\frac{\partial^2 F}{\partial x\partial y}. \tag{13}$$

Substituting these expressions in Eq. (6), we obtain

$$\nabla^4 F=E\left[\left(\frac{\partial^2 w}{\partial x\partial y}\right)^2-\left(\frac{\partial^2 w}{\partial x^2}\right)\left(\frac{\partial^2 w}{\partial y^2}\right)\right], \tag{14}$$

which is the first equation relating $w$and F. The second equation necessary to determine F and w is derived from the bending action [1] which is given by

$$\nabla^4 w=\frac{h}{D}\left[\frac{q}{h}+\left(\frac{\partial^2 F}{\partial y^2}\right)\left(\frac{\partial^2 w}{\partial x^2}\right)+\left(\frac{\partial^2 F}{\partial x^2}\right)\left(\frac{\partial^2 w}{\partial y^2}\right)-2\left(\frac{\partial^2 F}{\partial x\partial y}\right)\left(\frac{\partial^2 w}{\partial x\partial y}\right)\right]. \tag{15}$$

The transverse boundary conditions considered here are given by

$$BC_{w1}(w)=0 \text{ where } BC_{w1}(w)=w \text{ or } BC_{w1}(w)=V_n, \tag{16}$$

$$BC_{w2}(w)=0 \text{ where } BC_{w2}(w)=\frac{\partial w}{\partial n} \text{ or } BC_{w2}(w)=M_n, \tag{17}$$

where M_n and V_n are the normal bending moment and effective shear force that are given by

$$M_n = -D\left\{ v\nabla^2 w + (1-v)\left(n_x^2 \frac{\partial^2 w}{\partial x^2} + n_y^2 \frac{\partial^2 w}{\partial y^2} + 2n_x n_y \frac{\partial^2 w}{\partial x \partial y} \right) \right\}, \tag{18}$$

$$\begin{aligned} V_n = -D\Bigg\{ & \left(n_y\left(1-n_x^2(v-1)\right)\right)\frac{\partial^3 w}{\partial y^3} \\ & + n_x\left(-2n_x^2(v-1)+n_y^2(v-1)+v\right)\frac{\partial^3 w}{\partial y^2 \partial x} \\ & + n_y\left(n_x^2(v-1)-2n_y^2(v-1)+v\right)\frac{\partial^3 w}{\partial x^2 \partial y} \\ & + n_x\left(1-n_y^2(v-1)\frac{\partial^3 w}{\partial x^3}\right)\Bigg\}, \end{aligned} \tag{19}$$

where n_x and n_y are the x and y comonents of the unit vector normal to the boundary. The boundary conditions for the stress function F are obtained by assuming that the external edge of the plate is not subjected to inplane forces [1], which yields the following boundary conditions:

$$F = \frac{\partial F}{\partial n} = 0. \tag{20}$$

The solution of Eqs. (14) and (15), together with the boundary conditions (16)–(20), determines the two functions F and w. On having the stress function F, we can determine the stresses in the middle surface of a plate by applying Eqs. (10).

3. RBF formulation

Consider the 2-D computational domain (Fig. 1) that represents the plate geometry. For collocation, we use node points distributed both along the boundary $\left(\underline{x}_B^j, j = 1, ..., N_B\right)$, and over the interior $\left(\underline{x}_D^j, j = 1, ..., N_D\right)$. Let $\underline{x}_p = \{\underline{x}_B, \underline{x}_D\}$, so that the total number of points called poles is $N_p = N_B + N_D$. The deflection, w, is interpolated linearly by suitable RBFs:

$$\begin{aligned} w(\underline{x}) = & \sum_{j=1}^{N_D} \alpha_w^j \Phi\left(\left\|\underline{x} - \underline{x}_D^j\right\|\right) + \sum_{j=1}^{N_B} \beta_w^j BC_{w1}\left(\Phi\left(\left\|\underline{x} - \underline{x}_B^j\right\|\right)\right) \\ & + \sum_{j=1}^{N_B} \gamma_w^j BC_{w2}\left(\Phi\left(\left\|\underline{x} - \underline{x}_B^j\right\|\right)\right). \end{aligned} \tag{21}$$

Similarly, for the stress function F:

$$\begin{aligned} F(\underline{x}) = & \sum_{j=1}^{N_D} \alpha_F^j \Phi\left(\left\|\underline{x} - \underline{x}_D^j\right\|\right) + \sum_{j=1}^{N_B} \beta_F^j BC_{F1}\left(\Phi\left(\left\|\underline{x} - \underline{x}_B^j\right\|\right)\right) \\ & + \sum_{j=1}^{N_B} \gamma_F^j BC_{F2}\left(\Phi\left(\left\|\underline{x} - \underline{x}_B^j\right\|\right)\right), \end{aligned} \tag{22}$$

where $\Phi = \left\|\underline{x} - \underline{x}^j\right\|^n = r^n$ is a polynomial RBF of nth degree. Unlike the other RBFs, the polynomial RBF has the important advantage of being free of a shape factor which is a source of solution instability if not properly selected. It should be noted that there are some constraints on the permissible values of the polynomial degree n. This is explained by Table 1 that shows the results of the bi-harmonic operator ($\nabla^4\Phi$) for different degrees of the polynomial RBF, n. It is obvious that the usage of RBF polynomials with $n \leqslant 4$ for problems governed by the bi-harmonic operator such as the current problem yields either constant or singular values as $r \to 0$ and therefore these choices must be avoided. Furthermore, previous studies [13] have shown that even values of n produced inaccurate solutions. Therefore, we are left with odd values of $n \geqslant 5$. Few numerical experiments have been carried out to compare the accuracy of the solution of the linear plate problem for $n = 5$, 7 and 9. The results of these experiments have not shown any appreciable difference in terms of accuracy for $n = 5$ and 7. For $n = 9$, however, stability problems have been encountered, especially for high node intensities. Therefore, we have decided to use $n = 5$. The $4N_B + 2N_D$ unknown coefficients: α_w^j, β_w^j, γ_w^j, α_F^j, β_F^j and γ_F^j in Eqs. (21) and (22) can be determined by satisfying the governing equations and the corresponding boundary conditions at N_D domain points and N_B boundary points, respectively. The resulted equations can be expressed in the

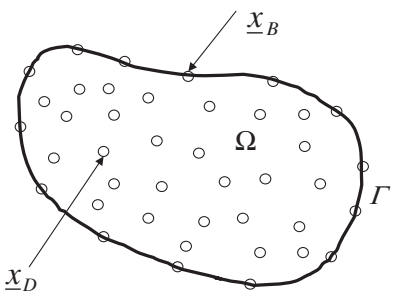

Fig. 1. Boundary and domain nodes.

Table 1
The bi-harmonic operator versus degree of RBF polynomial

n	$\nabla^4\Phi$
1	$1/r^3$
2	0
3	$9/r$
4	64
5	$225r$
6	$576r^2$
7	$1225r^3$
8	$2304r^4$
9	$3969r^5$

following matrix form:

$$\begin{bmatrix} BC_{w1}(\Phi) & BC_{w1}(BC_{w1}(\Phi)) & BC_{w1}(BC_{w2}(\Phi)) \\ BC_{w2}(\Phi) & BC_{w2}(BC_{w1}(\Phi)) & BC_{w2}(BC_{w2}(\Phi)) \\ \nabla^4\Phi & \nabla^4(BC_{w1}(\Phi)) & \nabla^4(BC_{w2}(\Phi)) \end{bmatrix} \begin{bmatrix} \alpha_w^i \\ \beta_w^i \\ \gamma_w^i \end{bmatrix} = \begin{bmatrix} 0 \\ 0 \\ \frac{h}{D}NL(w,F) \end{bmatrix} + \begin{bmatrix} 0 \\ 0 \\ \frac{q}{D} \end{bmatrix}, \tag{23}$$

$$\begin{bmatrix} \Phi & \Phi & \frac{\partial\Phi}{\partial n} \\ \frac{\partial\Phi}{\partial n} & \frac{\partial\Phi}{\partial n} & \frac{\partial}{\partial n}\left(\frac{\partial\Phi}{\partial n}\right) \\ \nabla^4\Phi & \nabla^4\Phi & \nabla^4\left(\frac{\partial\Phi}{\partial n}\right) \end{bmatrix} \begin{bmatrix} \alpha_F^i \\ \beta_F^i \\ \gamma_F^i \end{bmatrix} = \frac{E}{2} \begin{bmatrix} 0 \\ 0 \\ NL(w,w) \end{bmatrix}, \tag{24}$$

where

$$NL(w,F) = \left(\frac{\partial^2 F}{\partial y^2}\right)\left(\frac{\partial^2 w}{\partial x^2}\right) + \left(\frac{\partial^2 F}{\partial x^2}\right)\left(\frac{\partial^2 w}{\partial y^2}\right) - 2\left(\frac{\partial^2 F}{\partial x \partial y}\right)\left(\frac{\partial^2 w}{\partial x \partial y}\right), \tag{25}$$

and $NL(w,w)$ is obtained by replacing F by w in the foregoing expression.

4. Incremental-iterative procedure

In order to solve the above coupled and highly nonlinear equations, an incremental-iterative procedure is performed. In the following, the superscripts represent increments while subscripts represent iterations. As an example, the quantity $w^k_{i,xy}$ represents the second derivative of w with respect to x for the kth increment and ith iteration. Let us denote the number of increments by n. The following steps describe the incremental-iterative procedure:

(1) Apply the first load increment q/n and set the initial values of the second derivatives of w and F to zero, i.e. $F^1_{0,xx} = F^1_{0,yy} = F^1_{0,xy} = w^1_{0,xx} = w^1_{0,yy} = w^1_{0,xy} = 0$, so that $NL(w^1_0, F^1_0) = 0$ and Eq. (23) becomes

$$\begin{bmatrix} BC_{w1}(\Phi) & BC_{w1}(BC_{w1}(\Phi)) & BC_{w1}(BC_{w2}(\Phi)) \\ BC_{w2}(\Phi) & BC_{w2}(BC_{w1}(\Phi)) & BC_{w2}(BC_{w2}(\Phi)) \\ \nabla^4\Phi & \nabla^4(BC_{w1}(\Phi)) & \nabla^4(BC_{w2}(\Phi)) \end{bmatrix} \begin{bmatrix} \alpha_w \\ \beta_w \\ \gamma_w \end{bmatrix} = \begin{bmatrix} 0 \\ 0 \\ \frac{q/n}{D} \end{bmatrix}.$$

The above linear equations are then solved for the coefficients α_w, β_w and γ_w.

(2) Use the first estimates of α_w, β_w and γ_w in Eq. (21) to obtain the first estimate of deflection w^1_1. Note that w^1_1 corresponds to the solution of small-deflection theory for the first increment.

(3) Calculate $NL(w^1_1, w^1_1)$ and solve (24) for the first estimates of coefficients α_F, β_F and γ_F.

(4) Use first estimates for the coefficients α_F, β_F and γ_F in Eq. (22) to obtain the first estimate of the stress function F^1_1.

(5) Update the right hand side of (23) by calculating $NL(w^1_1, F^1_1)$ and solve for the updated values of the coefficients $f\alpha_w$, β_w and γ_w.

(6) Use Eq. (21) to obtain the second estimate of deflection w^1_2 and calculate $NL(w^1_2, w^1_2)$.

(7) Repeat the above steps until convergence is achieved, otherwise, decrease the load increment and repeat the iterations.

(8) Add the second load increment ($q = 2q/n$) and use the values obtained for $NL(w^1_n, F^1_n)$ at the last iteration of the first load increment, then repeat the above iterative procedure.

(9) Continue adding increments until the total load is applied.

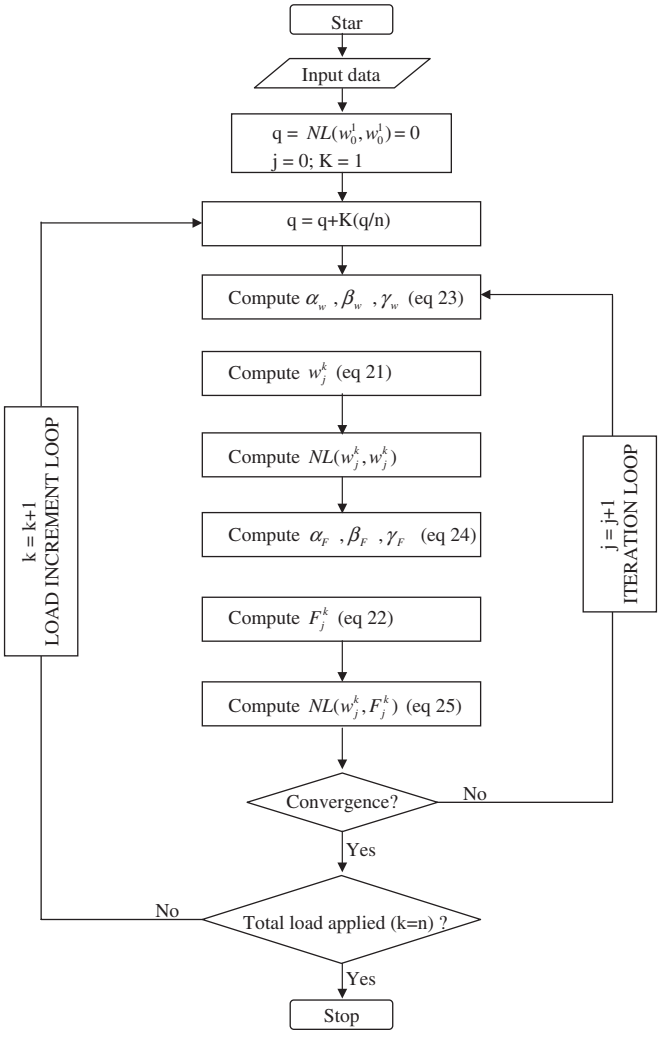

Fig. 2. Flow chart for the incremental-iterative procedure.

A flow chart representing the above algorithm is given in Fig. 2.

5. Numerical examples

In order to examine the effectiveness of the proposed RBF method for large deflection of thin plates, the following three examples are considered. The accuracy of RBF solutions are compared with the analytical and FEM solutions. All FEM solutions are obtained using the package ANSYS 9.0 [19]. In all examples, the load is assumed to be uniformly distributed $= q$, Poisson ratio v is assumed 0.3. For generality of the solutions, all quantities are made dimensionless, so that the coordinates, the load, the deflection and the stress are represented by $\bar{x} = x/a$, $\bar{y} = y/a$, $\bar{q} = qa^4/Eh^4$, $\bar{w} = w/h$ and $\bar{\sigma} = \sigma a^2/Eh^2$, respectively. In all examples, the load is increased until the central deflection exceeds 100% of the plate thickness.

Example 1. Consider a simply supported circular plate subjected to a uniformly distributed load $\overline{q}$ which is increased from 0.125 to 2 with equal increments of 0.125. The following approximate analytical solutions for the problem is given by Timoshenko [1]:

$$\bar{w}_c + A\bar{w}_c^3 = B\bar{q}, \tag{26}$$

$$\sigma_m = \alpha\bar{w}_c^2, \tag{27}$$

and

$$\sigma_b = \beta\bar{w}_c^2, \tag{28}$$

where $\bar{w}_c$ is central deflection, $\bar{\sigma}_m$ the stress in the plate middle plane (membrane stress), and $\bar{\sigma}_b$ the extreme fiber bending stress. The constants are $A = 0.262$, $B = 0.696$, $\alpha = 0.295$ and $\beta = 1.778$. The RBF and FEM solutions are obtained by employing a uniform nodal distribution consisting of 32 boundary nodes and 69 domain nodes as shown in Fig. 3. The evolution of the plate deflection at its plate center with the applied load is presented in Fig. 4 which reveals total agreement among RBF, FEM and the analytical solutions. The results for membrane and bending stresses at the center of the plate are given in Fig. 5 which shows excellent agreement between RBF and FEM solutions. The same figure shows deviations of both RBF and FEM solutions from the analytical solution especially for bending stress at higher loads. The deviations of the numerical solutions from the analytical solution can be attributed to the acknowledged inherent approximation of the analytical solution[1].

Example 2. Let us repeat example 1 by assuming a clamed edge boundary condition. The analytical solution is given by Eqs. (25)–(27), where $A = 0.146$, $B = 0.171$, $\alpha = 0.5$ and $\beta = 2.86$. The deflection and stress solutions of the problem are given in Figs. 6 and 7, respectively. The results for this example share the same observation of example 1 concerning the deviation of the numerical solutions from the analytical solution for the bending stress at high loads.

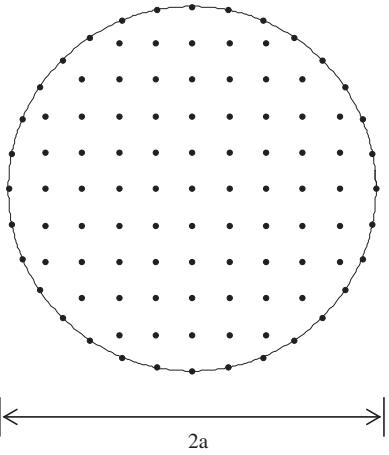

Fig. 3. Node distribution for Examples 1 and 2 ($N_B = 32$; $N_D = 69$).

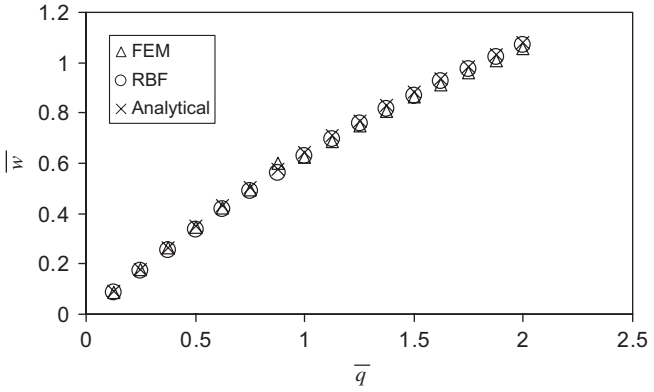

Fig. 4. Central deflection versus load for simply supported circular plate.

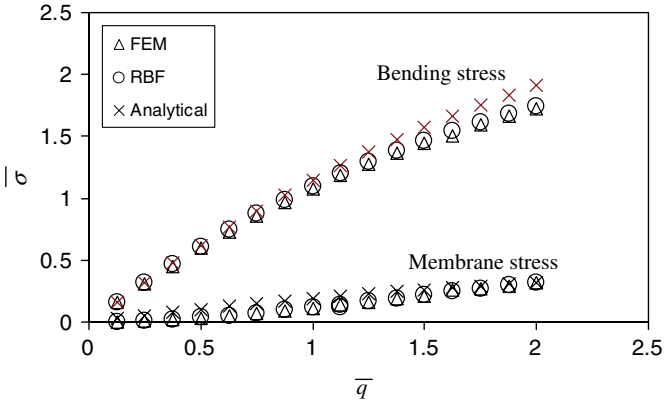

Fig. 5. Stresses at the center for simply supported circular plate.

Example 3. Consider a simply supported square plate subjected to a uniformly distributed load $\overline{q}$ which is increased from 2 to 32 with equal increments of 2. There is no analytical solution available for this problem and therefore the RBF solution is compared with FEM solution only. The problem is modeled using a uniform nodal distribution consisting of 36 boundary nodes and 81

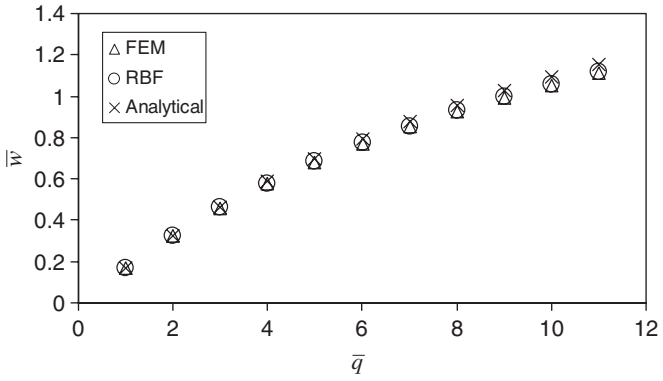

Fig. 6. Central deflection versus load for clamped circular plate.

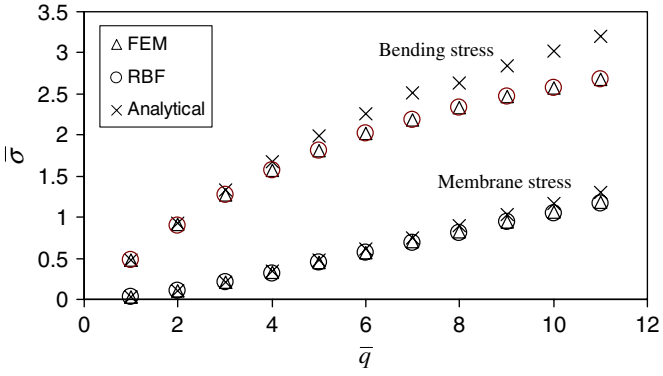

Fig. 7. Stresses at the center for clamped circular plate.

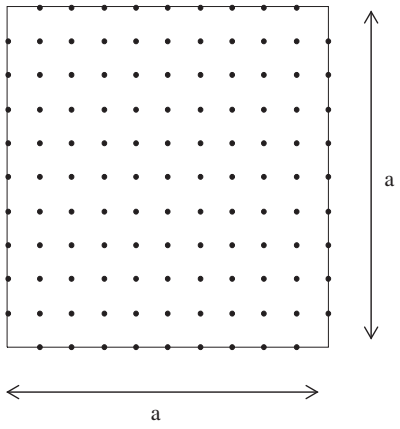

Fig. 8. Node distribution for Example 3 ($N_B = 36$; $N_D = 81$).

domain nodes as shown in Fig. 8. The results for maximum deflection and stresses are presented in Figs. 9 and 10, respectively. Both figures show excellent agreement between RBF and FEM solutions.

6. Conclusions

A simple meshless method for the analysis of thin plates undergoing large deflections is presented. The method is based on collocations with the fifth order polynomial radial basis function (RBF). This RBF does not require a shape

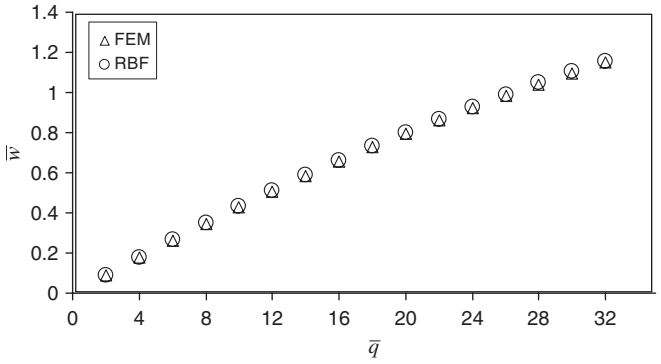

Fig. 9. Central deflection versus load for clamped square plate.

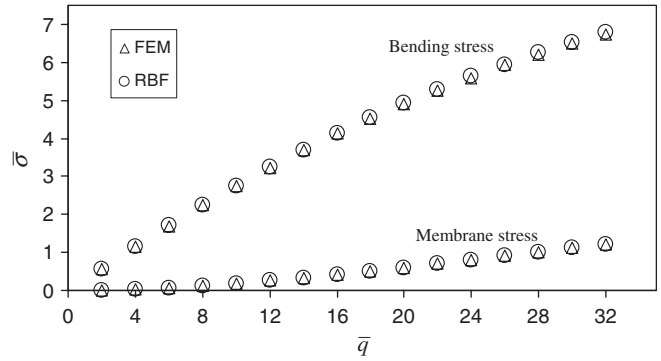

Fig. 10. Stresses at the center for clamped square plate.

parameter that needs to be specified as the case for other well-known RBFs. In addition, the method shares the same advantage of other RBF methods that do not require the computation of integrals or use of grids and meshes. The method can be easily extended to other nonlinear problems.

Acknowledgements

The authors would like to express their appreciation to King Fahd University of Petroleum and Minerals for supporting this study.

References

[1] Timoshenko SP, Woinowsky-Kreiger S. Theory of plates and shells. New York: McGraw-Hill; 1959.
[2] Augural C. Stresses in plates and shells. New York: McGraw-Hill; 1999.
[3] Little GH. Large deflections of rectangular plates with general transverse form of displacement. J Comput Struct 1999;71(3):333–52.
[4] Little GH. Efficient large deflections of rectangular plates with transverse edges remaining straight. J Comput Struct 1999;71(3):353–7.
[5] Ramachandra LS, Roy D. A novel technique in the solution of axisymmetric large deflection analysis of a circular plate. J Appl Mech 2001;68(5):814–6.
[6] Chen JT, Chen IL, Chen KH, Lee YT, Yeh YT. A meshless method for free vibration analysis of circular and rectangular clamped plates

using radial basis function. Eng Anal Bound Elements 2004;28(5):535–45.
[7] Vitor M. RBF-based meshless methods for 2D elastostatic problems. Eng Anal Bound Elements 2004;28(10):1271–81.
[8] Liew KL, et al. Mesh-free radial basis function method for buckling analysis of non-uniformly loaded arbitrarily shaped shear deformable plates. Comput Methods Appl Mech Eng 2004;193(3):205–24.
[9] Hardy RL. Multiquadric equations of topography and other irregular surfaces. Geophys Res 1971;176:1905–15.
[10] Nardini D, Brebbia CA. A new approach to free vibration analysis using boundary elements, boundary element methods in engineering. Southampton: Computational Mechanics Publications; 1982.
[11] Kansa EJ. Multiquadrics—a scattered data approximation scheme with applications to computational fluid-dynamics. I. Surface approximations and partial derivative estimates. Comput Math Appl 1990;19(8/9):127–45.
[12] Kansa EJ. Multiquadrics—a scattered data approximation scheme with applications to computational fluid-dynamics. I. Surface approximations and partial derivative estimates. Comput Math Appl 1990;19(8/9):147–61.
[13] Driscoll TA. Interpolation in the limit of increasingly flat radial basis functions. Comput Math Appl 2002;43(3):413–22.
[14] Ferreira AJM. A formulation of the multiquadric radial basis function method for the analysis of laminated composite plates. Compos Struct 2003;59:385–92.
[15] Ferreira AJM, Roque CMC, Martins PALS. Radial basis functions and higher-order theories in the analysis of laminated composite beams and plates. Compos Struct 2004;66:287–93.
[16] Ferreira AJM. Polyharmonic (thin-plate) splines in the analysis of composite plates. Int J Mech Sci 2005;46:1549–69.
[17] Ferreira AJM. Free vibration analysis of Timoshenko beams and Mindlin plates by radial basis functions. Int J Comput Methods 2005;2(1):15–31.
[18] Larsson E, Fornberg B. Theoretical and computational aspects of multivariate interpolation with increasingly flat radial basis functions. Comput Math Appl 2005;49:103–30.
[19] Ansys Inc. ANSYS 9.0 Documentation, 2005.